

Strength-Probability-Time Diagrams using Power Law and Exponential Kinetics Models for Fatigue

M. John Matthewson*

Department of Materials Science & Engineering, Rutgers, The State University of New Jersey,
607 Taylor Road, Piscataway, NJ USA 08854-8065

ABSTRACT

Strength-Probability-Time (SPT) diagrams provide an intuitively pleasing method for presenting reliability data based on extrapolations from accelerated fatigue testing data. If power-law crack growth kinetics are assumed the calculations required to generate the SPT diagram are particularly simple. However, if exponential or other more complex forms are used, this is not the case. If the accelerated data are for dynamic fatigue measurements (strength as a function of stressing rate) the SPT diagram can only be determined after numerical integration of the crack growth equations, followed by non-linear regression to the fatigue data. However, we have developed software to perform this task. In this paper we describe the methods used and show sample results of lifetime predictions using SPT diagrams. Also, the effect of using different crack growth kinetics models on predicted lifetimes is discussed.

Keywords: Optical fiber, strength, fatigue, SPT diagram, subcritical crack growth, kinetics, reliability.

1. INTRODUCTION

The mechanical reliability of optical fiber and of many fiber components is normally assured by proof testing which removes the largest defects so that the surviving fiber or components have a minimum assured strength. Standard fatigue equations based on power law crack growth kinetics are then used to predict the minimum time to failure for a given applied service stress, or to calculate the maximum permitted service stress that ensures a specified service life. Although simple in principal, the equations are complicated by accounting for subcritical crack growth during proof testing and during unloading after the proof test. The equations are further complicated when two region power law crack growth is taken into account [1]. However, mathematical models are published and guidelines for service stress or lifetime calculations as a function of proof stress are available [1].

Many fiberoptic components using lengths of fiber require removal of the polymer coating from the fiber thus exposing the fragile glass surface to damage during subsequent fabrication steps. Proof testing the fiber prior to fabrication is not useful because the fabrication process might well introduce damage into the fiber surface. Proof testing after encapsulation might also not be feasible since the fiber might be bonded or strain relieved where it enters the package. Therefore, for some fiberoptic components it is not possible to proof test the fiber and so ensure a minimum strength. In such cases it is therefore hard to ensure mechanical reliability; unless it can be assured that the fiber sees no mechanical stress (which is usually not the case). However, in some cases it is possible to dismantle the component and carefully remove the fiber and then measure its strength. Also, it might be possible to remove the fiber before final assembly, provided that final step itself can not introduce damage. This permits characterization of the strength distribution of the fiber which in turn can be used for making lifetime predictions. Such predictions are probabilistic since without proof testing there is no assured minimum strength and the minimum strength for any component can in principal be arbitrarily small. However, a probabilistic estimate of reliability is better than no estimate at all.

Optical fiber components for which this approach may apply include certain designs of connectors, couplers, fiber Bragg gratings, amplifiers, sensors, *etc.*. We are unaware of any published data on the strength of fiber extracted from such components; measurements have either not be performed or, more likely, the information is of a highly sensitive, proprietary nature. This work will therefore illustrate the kinds of reliability predictions that can be made by using

* mjohnm@fracture.rutgers.edu; phone & fax +1-732-445-5933; www.rutgers.edu/~mjohnm

published data for fiber that has been deliberately weakened by methods which model typical strength degrading processes such as handling of bare fiber.

2. CALCULATION OF STRENGTH-PROBABILITY-TIME DIAGRAM

Strength-Probability-Time (or SPT) Diagrams [2] are a useful tool for visualizing reliability data. It is assumed that the fiber removed from a component is broken under conditions of dynamic fatigue (constant stress rate) at one or more stress rates. This permits estimation of the flaw size/strength distribution and in addition, if multiple stress rates are used, estimation of the stress corrosion susceptibility parameter, n . If only one stress rate is used then a worst case value for n will need to be assumed. Starting with the measured strength distribution, it is possible to predict the static fatigue behavior, *i.e.* the distribution of, for example, the time to failure for a given service stress or of failure stress for a given design life. SPT diagrams are a graphical representation of the results of such calculations.

2.1 Calculation of SPT diagrams for power law fatigue kinetics

Calculation of SPT diagrams is normally performed by a sequence of steps that involve using the well-known result that for power law fatigue the time to failure in dynamic fatigue (constant stress rate) is $(n+1)$ times greater than the time to failure in static fatigue (constant applied stress) for the same stress at failure (*e.g.* Ref. 3). However, a more straightforward approach is to combine the static and dynamic fatigue equations. It is useful to summarize the derivation of the relevant equations so that the built-in assumptions are made clear. Power law fatigue is assumed, *i.e.* the crack growth rate, $v = dc/dt$, is proportional to a power of the stress intensity at the crack tip, K_I :

$$v = AK_I^n, \quad (1)$$

where A and n are fit parameters. This equation is combined with the standard fracture mechanics equation that relates the stress intensity due to an applied stress σ acting on a crack of length c and shape parameter, Y :

$$K_I = Y\sigma c^{1/2}, \quad (2)$$

to generate a differential equation that can be solved for any loading scheme, $\sigma(t)$. For static fatigue the applied stress is constant, $\sigma(t) = \sigma_a$, giving the time to failure:

$$t_f = \frac{2}{(n-2)AY^2\sigma_a^n K_{IC}^{n-2}} \left(\sigma_i^{n-2} - \sigma_a^{n-2} \right), \quad (3)$$

where σ_i is the initial or inert strength defined by:

$$K_{IC} = Y\sigma_i c_i^{1/2}, \quad (4)$$

where c_i is the initial length of the crack. The applied stress is normally somewhat less than the inert strength so that, given that n is usually large (typically greater than or about 20 for silica):

$$\sigma_a^{n-2} \ll \sigma_i^{n-2}. \quad (5)$$

The second term in parentheses in equation (3) is therefore negligible so that, to a good approximation, equation (3) simplifies to the well-known result:

$$t_f = \frac{2}{(n-2)AY^2\sigma_a^n} \left(\frac{\sigma_i}{K_{IC}} \right)^{n-2}, \quad (6)$$

or

$$t_f = B \frac{\sigma_i^{n-2}}{\sigma_a^n}, \quad (7)$$

where the “ B parameter” is:

$$B = \frac{2}{(n-2)AY^2K_{IC}^{n-2}}. \quad (8)$$

A similar approach may be taken for the case of dynamic fatigue with a constant stress rate, $\sigma(t) = \dot{\sigma}t$. The strength or failure stress, σ_f , is given by:

$$\sigma_f^{n+1} = \frac{2(n+1)\dot{\sigma}}{(n-2)AY^2K_{IC}^{n-2}} \left(\sigma_i^{n-2} - \sigma_f^{n-2} \right). \quad (9)$$

Usually the strength σ_f is measured at moderate rates so that it is significantly smaller σ_i and so again, given that n is usually large:

$$\sigma_f^{n-2} \ll \sigma_i^{n-2}. \quad (10)$$

The second term in parentheses in (9) is therefore negligible giving:

$$\sigma_f^{n+1} = (n+1)\dot{\sigma}B\sigma_i^{n-2}. \quad (11)$$

The term in $B\sigma_i^{n-2}$ cancels when equations (7) and (11) are divided together to give:

$$\sigma_a^n t_f = \frac{\sigma_f^{n+1}}{(n+1)\dot{\sigma}}. \quad (12)$$

Equation (12) can be used to construct an SPT diagram directly. For each strength measurement taken at various stressing rates, $\sigma_f(\dot{\sigma})$, the corresponding time to failure t_f can be determined for a given service stress, σ_a . This results in a distribution of times to failure for that service stress, or alternatively, the distribution of failure stresses for a given service life can be calculated.

The above analysis is well known and has been published in textbooks [3]. However, it is outlined in detail here for the following reason. Equation (12) is very convenient since it does not require knowledge of σ_i , which is a parameter that is hard to measure accurately (*e.g.* Ref. 4). But, this is only the case if it is possible to use the approximations of equations (5) and (10). If any measurement under static or dynamic conditions exposes the fiber to a stress close to the initial/inert strength, σ_i , those approximations are invalid and so equation (12) is also invalid. Under these circumstances, a value for σ_i (but not B) is needed for calculation of SPT diagrams. This is demonstrated by dividing equations (3) and (9) to yield:

$$\frac{t_f}{\sigma_f^{n+1}} = \frac{1}{(n+1)\dot{\sigma}\sigma_a^n} \frac{\left(\sigma_i^{n-2} - \sigma_a^{n-2} \right)}{\left(\sigma_i^{n-2} - \sigma_f^{n-2} \right)}. \quad (13)$$

However, equation (13) is invalid due to another assumption/approximation that is implicit in the above derivations.

It was implicitly assumed that equation (1) is valid throughout the region of interested, *i.e.* for values of K_I ranging from its initial value at the start of a measurement to K_{IC} when the crack starts growing unstably. It has been shown [5] that weak silica optical fiber exhibits “Region II” subcritical crack growth in addition to the “Region I” behavior described by equation (1). This will influence the behavior if the fiber is ever subjected to stresses comparable to σ_i ; this is the case when proof testing and Glaesemann and co-workers have incorporated this behavior into reliability models for fiber that has been proof tested [1].

Notwithstanding this, if the approximations of equations (5) and (10) are valid (and this is usually the case) σ_i does not need to be known. Essentially this is because the time that the crack spends exposed to K_I near K_{IC} is negligible

compared to the overall time to failure and so the actual behavior in that region is unimportant. In particular, the presence of Region II subcritical crack growth is not relevant. This has important implications for the calculation of the SPT diagram for exponential kinetics models. Further justification for this statement will be provided later.

2.1 Calculation of SPT diagrams for exponential fatigue kinetics

The power law form of the kinetics for fatigue, equation (1), is empirical and is not based on any physical model. It is used principally for its mathematical simplicity. When combined with the fracture mechanics relationship the resulting differential equation can be integrated to produce analytical results for both static and dynamic fatigue. For more convenient comparison with other kinetics models, the power law will be referred to as Model 1 and the fatigue parameters, A and n , will be represented by a subscript one. Equation (1) then becomes:

$$v = A_1 K_I^{n_1}, \quad (14)$$

Exponential forms have been proposed that are based on chemical rate theory. Model 2 was suggested when it was first recognized that fatigue is a stress corrosion phenomenon [6]:

$$v = A_2 \exp(n_2 K_{IC}). \quad (15)$$

This form assumes that the crack tip stress affects the chemical kinetics through an activation volume in much the same way that pressure is known to affect chemical kinetics. A more rigorous treatment yields a form [7] which can be simplified to give Model 3 [8]:

$$v = A_3 \exp(n_3 K_{IC}^2). \quad (16)$$

All three models that we consider here have two parameters, A_i and n_i ($i = 1..3$), which have similar meaning. The n_i represent the sensitivity of the crack growth rate to the stress intensity at the crack tip while the A_i are a measure of the overall rate and are related to, for example, the activity of moisture (humidity). All three models can be interpreted in terms of absolute rate theory for the stress corrosion process in which case the n_i represent how the activation barrier for the reaction is reduced by stress [9]. The n_i are not constants but depend on temperature [10].

Of the three models considered here it is unclear which one is correct to use. For pristine fiber the power law gives a better fit to fatigue data but the exponential model gives a more consistent view of the effect of environment [9]. There is less information available for weak fiber, probably because the increased scatter leads to inconclusive results (as is the case for the data considered here). However, there is evidence from slow crack growth measurements that the simple exponential form of equation (15) gives a better description than the other two [11,12]. Certainly, there is no evidence that Model 3, equation (16), fits any data best which is encouraging since it gives very pessimistic lifetime predictions. While the power law is ubiquitous in the fiber optics industry, Model 2 might be a more prudent choice for critical applications if a truly "worst case" assessment is sought.

While the exponential models are more physically reasonable than the power law, they are mathematically substantially less convenient to use. In particular, the case of dynamic fatigue can not be solved analytically and numerical methods are required. As a result the calculation of SPT diagrams is significantly more complex than simply substituting experimental results into a simple equation such as equation (12). The question is then how to perform the calculations needed to generate the SPT diagram?

SPT diagrams are Weibull plots that represent the variability expected in the static fatigue behavior. This variability results fundamentally from variability in the size of the defect or crack that leads to failure, *i.e.* it results from the variability in the inert strength. It is therefore proposed that the SPT diagram can be calculated via calculations of inert strength. However, as discussed above, the inert strength is difficult to measure. This difficulty is avoided by assuming a reasonable value for the central or average inert strength. Since the mapping from dynamic to static fatigue is insensitive to the inert strength, the actual value assumed is unimportant, as will be shown.

Calculations that are used here involve integration of the kinetics equations, (15) or (16), using an appropriate loading scheme (constant stress or constant stress rate). A fourth order Runge-Kutta method has been used. Precision has been

verified by comparing the numerical results for static fatigue to the analytical results which are available. The SPT diagram is then calculated using the following steps:

1. Fit to the measured dynamic fatigue data using an assumed reasonable value for the average inert strength to obtain the best fit fatigue parameters, A_i and n_i . Nonlinear least squares regression is used for this purpose [13]. Although not needed for the SPT calculations, confidence intervals for the fatigue parameters are determined taking into account their correlations [13].
2. For each measurement of strength at each stress rate, the fatigue equation is integrated using the best fit values of A_i and n_i while the inert strength is iteratively adjusted (using a Newton-Raphson algorithm) until the calculated strength matches the actual measurement. In effect this back-calculates the inert strength corresponding to each strength measured under dynamic fatigue conditions. The result of this step is a distribution of inert strengths.
3. For each inert strength determined in the previous step, the fatigue equation is integrated under static fatigue conditions to obtain the time to failure for a given applied stress. Alternatively, the applied stress is iteratively adjusted (again using a Newton-Raphson algorithm) to obtain the applied stress that results in a given time to failure. The results of this step are graphed as a Weibull plot which is the needed SPT diagram.

The numerical methods used were verified by comparing the results of numerical calculations for the power law with those calculated using equation (12). The analytical and numerical results were essentially indistinguishable.

3. RESULTS

The methods developed here for determining SPT diagrams for the exponential kinetics have been illustrated by applying them to data for weak fiber that have been published in the literature. Yuce *et al.* [14] made deliberately weakened fiber by passing it over an abrasive coated wheel on-line during the draw process prior to coating. They then measured the dynamic fatigue of the fiber both as-received and after aging for various times in different environments. For the unaged as-received fiber they measured the strength of 60 specimens at each of four strain rates each separated by a decade in rate. They show a Weibull plot (their figure 3) on which the points show considerable overlap and which can not be individually resolved. This figure has been digitized and the results have been interpolated to generate 15 measurements at each rate to give dynamic fatigue measurements that are compliant with the widely used standard test procedure, FOTP-28 [15]. This approach therefore approximates a random subset of the original data. Figure 1a shows a Weibull plot of the resulting data; the Weibull modulus is approximately 5. Figure 1b shows a log-log dynamic fatigue plot for these data where the points are the (geometric) mean of the data for each rate and the error bars are a

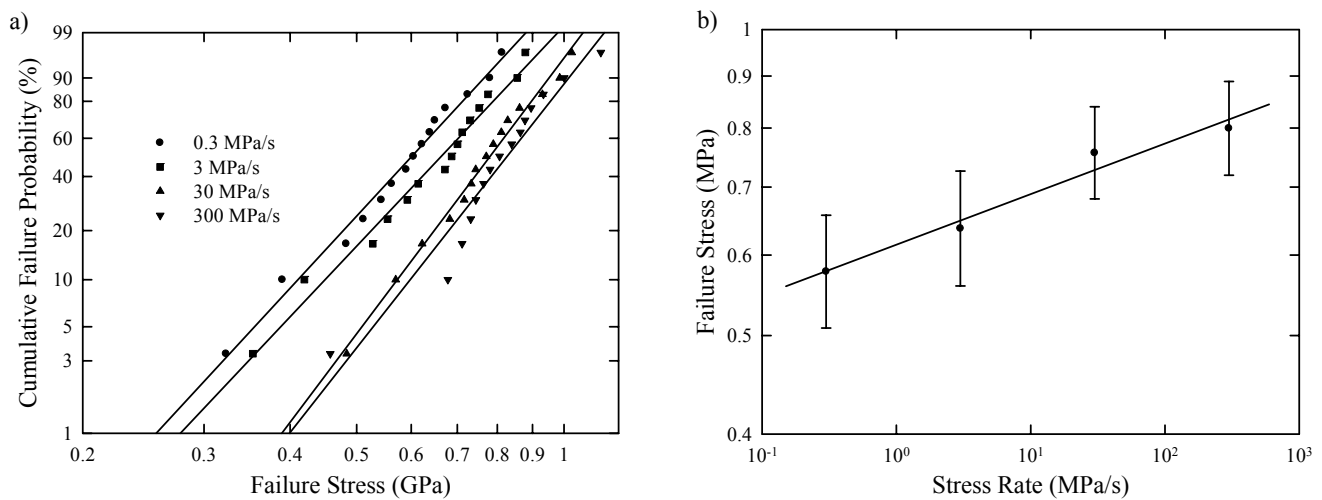


Fig. 1. (a) Weibull plot and (b) dynamic fatigue plot of a subset of the data of Yuce *et al.* [14] for deliberately weakened fiber.

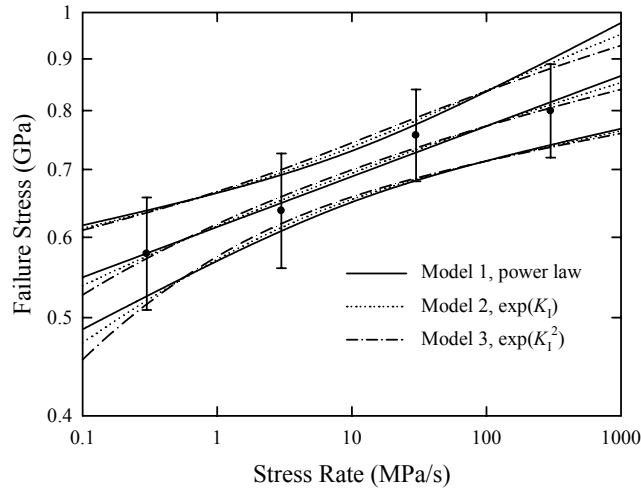


Fig. 2. Fits of the three crack growth kinetics models to the data of figure 1. The confidence bands represent a 95% interval.

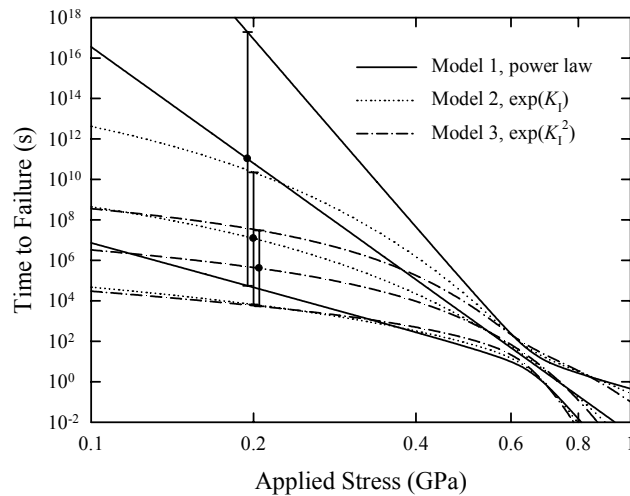


Fig. 3. Predictions of static fatigue behavior using the fatigue parameters found by fitting to the dynamic fatigue data of figure 2.

95% confidence interval for the mean. The solid line is found by fitting the power law fatigue equation (11) to the data using methods specified in FOTP-28. From the slope of the line the fatigue parameter n is found to be 19 with a 95% confidence interval from 13 to 36. A value of 19 is perhaps a little low but not untypical and the rather broad confidence interval results from the large scatter in the data.

Figure 2 shows the results of fitting the three kinetics models to the same data using nonlinear regression coupled with numerical integration of the dynamic fatigue equations. Also shown are the 95% confidence bands for the regression fit. It is found that none of the three models gives a significantly better fit than the others, principally because of the large scatter in the data.

Figure 3 shows the predicted static fatigue behavior of the fiber using the best fit parameters and their variances. As is well known, the exponential forms predict a much shorter lifetime at low applied stress than the power law [8,16]. Interestingly, the lower bound of the 95% confidence interval does not show such a big difference between the models. The confidence intervals for the predictions are large (as exemplified by the error bars for an applied stress of 0.2 GPa) which is unremarkable given the scatter in the data. However, there have been several studies of the fatigue of weak fiber so that there is more knowledge about the behavior than simply given by the data used here. A review [17] of the

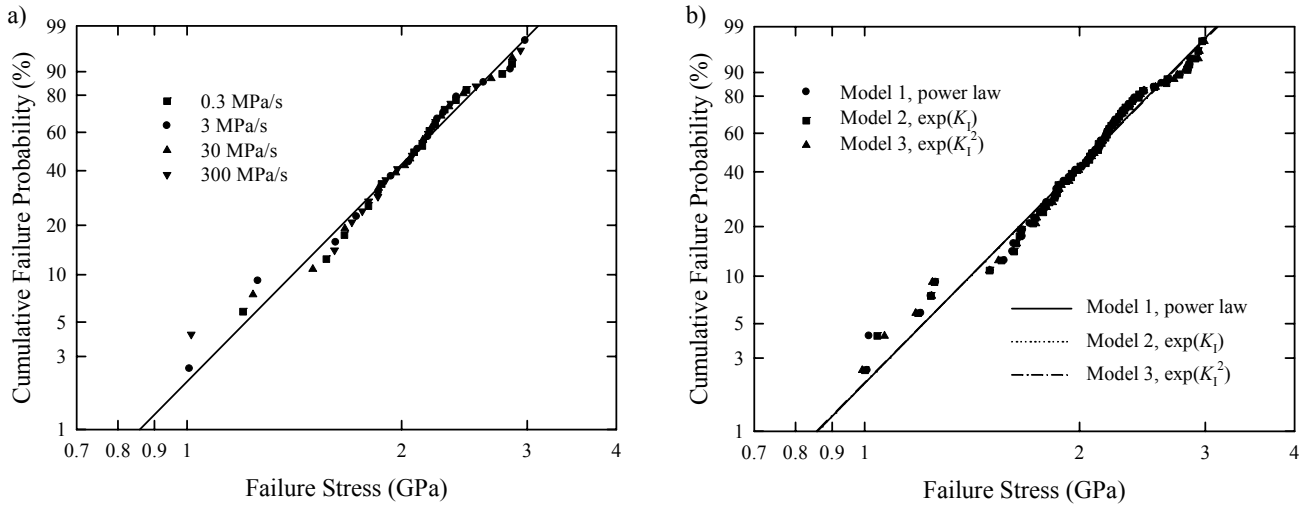


Fig. 4. Inert strengths calculated from the dynamic strengths in figure 1a using a mean inert strength of 2 GPa; (a) results for the power law showing different stress rates and (b) results for all three kinetics models.

power law exponent, n or n_1 , for weak fibers shows literature values lying between approximately 20 and 40. Although there have been several other studies since that review was published, they have not changed that picture. Therefore the best fit value of $n = 19$ might be considered, in the light of other studies, as a suitable “worst case” value so that the lower confidence bound in figure 3 is overly pessimistic. In practical situations in which fiber can not be proof tested, there might be insufficient specimens to determine the fatigue behavior so only a strength measurement at a single rate is available. Lifetime predictions then have to use a worst case n obtained from other work and the solid lines in figure 3 then might be considered as a more realistic worst case for the example data being considered here.

As prescribed above, the intermediate step in calculating the SPT diagrams is calculating the inert strength corresponding to each strength measurement and the results are shown in figure 4. The results were calculated assuming a value for the average inert strength of $\sigma_i = 2$ GPa which is roughly three times the mean measured strength (figure 1). Figure 4a shows results calculated for the power law only; the different symbols correspond to different stress rates and it is observed that the inert strengths for each rate are distributed approximately uniformly across the Weibull plot. This means that the fatigue parameters found by fitting to the original strength data are correct – if they were not, the inert strengths corresponding to each rate would be grouped together and not uniformly spread out. Figure

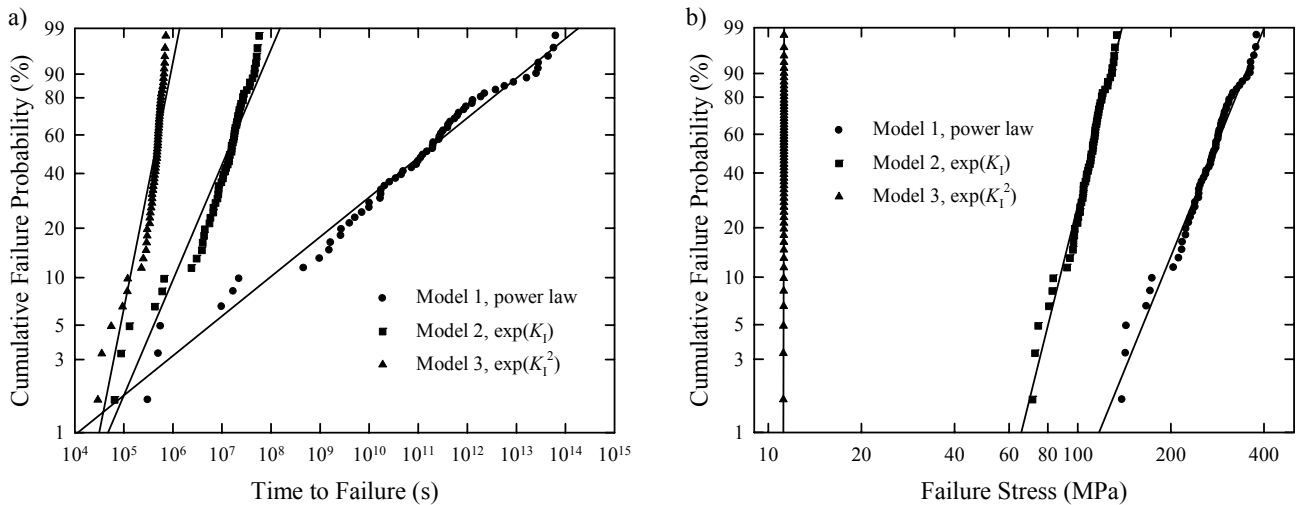


Fig. 5. SPT diagrams calculated from the inert strengths shown in figure 4b; (a) distribution of failure times for an applied stress of 200 MPa, (b) distribution of failure stresses for a 10 year time to failure.

4b shows the results for both the power law and the exponential forms. The data for the different models are, of course, centered in the same position because the same value of average inert strength is assumed in all three cases. However, the data are very similar and the distribution widths are similar. Indeed, the fit lines, which are the Weibull distribution estimated by an unbiased likelihood technique [18], are almost coincident for all three kinetics models. Overall, therefore, the calculated inert strengths are insensitive to the assumed form of the kinetics model.

The inert strengths are then used to calculate the predicted static fatigue behavior, *i.e.* the SPT diagrams corresponding to the original data. Examples of two types of SPT diagram are shown in figure 5. Figure 5a is a Weibull plot of the calculated failure times for a 200 MPa applied/service stress. The alternative view in figure 5b shows the calculated failure stresses for a 10 year lifetime; this diagram can be used to read off the probability of failure during the design life for any given service stress.

As expected, both figures predict poorer performance using the exponential forms than the power law; shorter lifetimes for a given service stress or higher probability of failure for a given service life. However, another feature is that the distribution widths are substantially narrower for the exponential forms. This can be qualitatively understood from what is known about the statistics for the power law. Assuming power law kinetics, the Weibull modulus for the time to failure under a static stress, m_s , is related to the Weibull modulus of strength measurements under dynamic fatigue, m_d , via the power law fatigue parameter, n , [3]:

$$m_s = \frac{1}{n+1} m_d \approx \frac{1}{n} m_d. \tag{17}$$

This means that for smaller values of n the Weibull modulus of the times to failure is higher and hence there is less scatter. n can be defined in terms of the slope of the static fatigue plot:

$$n = - \frac{d \log t_f}{d \log \sigma_a} \tag{18}$$

It is seen from figure 3 that the effective power law n , at for example 200 MPa applied stress, is lower for the exponential forms than for the power law since the slopes are shallower. Equation (17) therefore suggests that the scatter in the predicted times to failure should be lower for the exponential forms, as is indeed observed in figure 5.

The width of the distributions in figure 5 represents uncertainty in the behavior of a single specimen. This does not include the uncertainty due to the error in the estimates of the fatigue parameters, A_i and n_i . The confidence bands for the extrapolations in figure 3, however, do characterize that effect. Taking a service stress of 200 MPa as an example, the confidence bands in figure 3 can be superimposed on the SPT diagram as shown in figure 6, where the error bars are

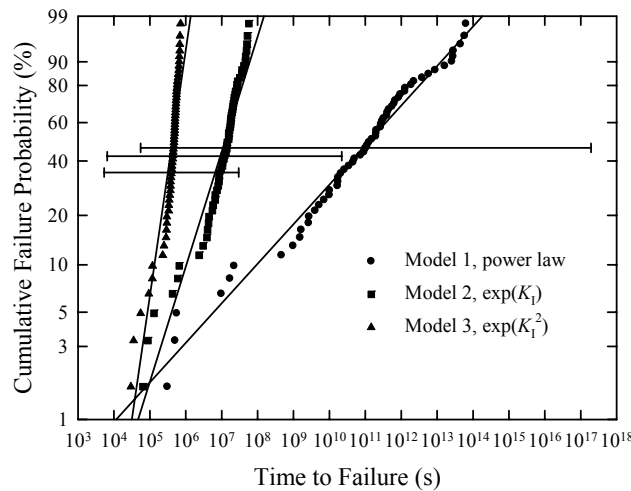


Fig. 6. SPT diagram of figure 5a with confidence bands for the extrapolation for the mean lifetime determined from figure 3.

centered on the (geometric) average time to failure. In this way we can compare the variability about the mean due to (i) the extrapolation error and (ii) the intrinsic scatter in the strength. These two quantities are somewhat related but are not the same. For the data examined here the 95% error bars on the extrapolation are wider than the distribution. In this particular case it means that uncertainty in the extrapolated mean time to failure is dominated by uncertainty in the fatigue parameters, rather than the intrinsic scatter in the strength. The uncertainty in the predicted lifetime tends to be controlled by uncertainty in the fatigue parameter for longer times to failure and narrower strength distributions

It was argued earlier that the details of the v - K_I behavior in the region of the inert strength makes no difference to the results even though those results are obtained by calculating the inert strength. Confirmation of this can be obtained by changing the assumed mean inert strength. Figure 6 was calculated assuming a mean inert strength of 2 GPa; using values of 1.5 and 2.5 GPa changed the results by less than 0.1% for all the data points for all three models. Since the assumed inert strength does not change the SPT diagram, it is reasonable to assume that if there is a change in behavior in the region of the inert strength, *e.g.* if Region II crack growth occurs, this will also not significantly change the results.

3.1 Effect of the strength distribution

While the SPT diagrams are typically plotted with a Weibull probability scale, the method for obtaining the data does not assume a Weibull distribution, or indeed any other particular distribution. Analytical models for reliability do need to make some assumption about the mathematical form of the inert strength distribution which can be a disadvantage.

Breuls and Svensson [19] made weak optical fiber by drawing the fiber from a preform whose surface had been deliberately contaminated with zirconia particles. They found that a Weibull plot of the strengths showed distinct non-linearity and was not described well by the Weibull distribution. They attributed this effect to the zirconia particle size distribution. Their data are reproduced in figure 7a where it is seen that the shape of the distribution is similar for each of four stress rates. These data have been used to construct an SPT diagram for static fatigue subjected to a service stress of 250 MPa and the result is seen in figure 7b. The non-linear shape of the distribution is reproduced in the SPT diagram, although it is less obvious for the exponential forms because of their narrow width. This result illustrates that the SPT diagram faithfully reproduces the shape of the strength distribution even if it is not a simple Weibull distribution.

3.2 Effect of the service environment

The analysis in section 2 above implicitly assumes that the fatigue constants, A_i and n_i , are indeed constant. This

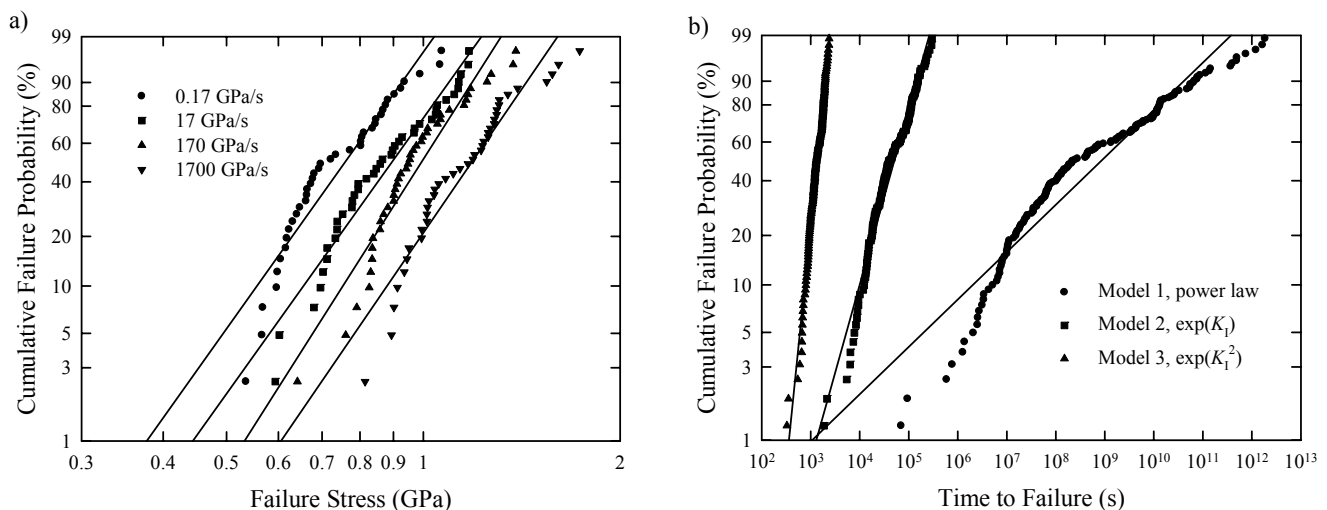


Fig. 7. (a) Dynamic fatigue data of Breuls and Svensson [19] and (b) SPT diagram calculated for an applied stress of 250 MPa.

therefore assumes that the test environment for the dynamic fatigue measurements is the same as the service environment. In cases where this is not so, the SPT diagrams can still be calculated if it is known how the fatigue parameters vary with environment. The procedure is to calculate the inert strengths using the fatigue parameters found by fitting to the dynamic fatigue data. The SPT diagram is then calculated from the inert strengths using fatigue parameters appropriate for the service environment. The behavior of the fatigue parameters is known in some detail for pristine fiber as a function of temperature, humidity and pH [9], but much less is known for weak fiber.

3.3 Effect of test technique and fiber length

The distribution of stress in the fiber may well be different in service and while strength testing. For example, a fiber amplifier might comprise a coil of fiber which experiences a bending stress while the strength measurement would normally be conducted in uniaxial tension. The effective lengths of fiber subjected to stress would be different in these two cases. This can be taken into account using suitable “shape factors” [3]. Shape factors are normally determined assuming both a Weibull distribution and power law fatigue. The most commonly encountered stress distributions are uniaxial bending, uniform (mandrel) bending and two-point bending. Shape factors for two-point bending have been found for both static and dynamic fatigue and have been compared to tension and uniform bending [20,21].

Once the shape factors are known it is relatively straightforward to incorporate their effect into the SPT diagram calculations. First the SPT diagram is determined using the methods outlined above. This results in a Weibull plot of the times to failure for the same stress distribution as the strength measurements (*i.e.* uniaxial tension for the amplifier example). The Weibull modulus of the static time to failure is then calculated from the data. Next, the results are corrected for the change in stress field by applying the appropriate shape factor. The shape parameter is usually a simple factor which depends only on the Weibull modulus of the static fatigue case; as such it represents a sideways or vertical shift of the data in the SPT diagram.

4. CONCLUSIONS

Ideally, the reliability of optical fiber and fiber components should be assured by proof testing. However, in some situations this is not possible, for example when a fiber is enclosed in a device with strain relief which forbids the possibility of applying any proof stress. In such circumstances the reliability can only be assured if it is assured that the fiber is not subjected to any stress – but this is usually not possible. It may, however, be possible to remove fiber from some devices and measure its strength to characterize the strength distribution, and perhaps also to characterize the fatigue characteristics. Stress-Probability-Time diagrams can then be used to predict failure rates for a given service stress or service life.

A method for calculating Stress-Probability-Time diagrams for assessing optical fiber reliability has been proposed here which involves using the inert strength corresponding to each measured strength as an intermediate step. The methodology has been successfully applied to literature data for relatively weak fiber. As expected, the power law makes the most optimistic prediction of performance while the physically more reasonable exponential forms give a more conservative view. In addition it is found that the widths of the predicted distributions of time to failure or failure stress for long-term behavior are quite different for the different kinetics models – the distribution is widest for the power law. Methods are given for accounting for differences between the service and testing environments and differences between the service and testing stress distributions.

SPT diagrams are a useful way of visualizing reliability behavior. In particular they enable one to directly visualize the distribution of failure times for a given service stress (or failure stresses for a given service life) and so take into account variability in lifetime due to the inherent variability in strength. However, they do not account for uncertainty in the fatigue parameters used to make the predictions, but this source of uncertainty might dominate. SPT diagrams do not therefore give all the information needed for making reliability predictions but are a useful adjunct to other methods. They are particularly useful if “worst case” values for the fatigue parameters are used since parameter uncertainty is then not an issue.

REFERENCES

1. T. A. Hanson and G. S. Glaesemann, "Incorporating multi-region crack growth into mechanical reliability predictions for optical fibres," *J. Mat. Sci.* **32** 5305-5311 (1997).
2. R. W. Davidge, J. R. McLaren and G. Tappin, "Strength-probability-time (SPT) relationships in ceramics," *J. Mat. Sci.* **8** [12] 1699-1705 (1973).
3. J. B. Wachtman, *Mechanical properties of ceramics*, Wiley, New York (1996).
4. G. S. Glaesemann and J. D. Helfinstine, "Measuring the inert strength of large flaws in optical fiber," *Proc. Soc. Photo-Opt. Instrum. Eng.* **2074** 95-107 (1993).
5. P. T. Garvey, T. A. Hanson, M. G. Estep and G. S. Glaesemann, "Mechanical reliability predictions: an attempt at measuring the initial strength of draw abraded optical fiber using high stress rates," *Proc. 46th Int. Wire & Cable Symp.* 883-887 (1997).
6. R. J. Charles and W. B. Hillig, "The kinetics of glass failure by stress corrosion" in "Symposium sur la resistance mecanique du verre at le moyens d l'ameliorer," Anonymous p. 511, Union Sciences Continentale du Verre, Charleroi, Belgium, (1962).
7. B. R. Lawn, "An atomistic model of kinetic crack growth in brittle solids," *J. Mat. Sci.* **10** 469-480 (1975).
8. K. Jakus, J. E. Ritter, Jr. and J. M. Sullivan, "Dependency of fatigue predictions on the form of the crack velocity equation," *J. Am. Ceram. Soc.* **64** [6] 372-374 (1981).
9. M. J. Matthewson, "Environmental effects on the fatigue and lifetime predictions for silica optical fibers," *Proc. Soc. Photo-Opt. Instrum. Eng.* **4940** 80-92 (2003).
10. M. J. Matthewson, "Chemical kinetics models for the fatigue behavior of fused silica optical fiber," *Mat. Res. Soc. Symp. Proc.* **531** 143-153 (1998).
11. M. Muraoka and H. Abé, "Subcritical crack growth in silica optical fibers in a wide range of crack velocities," *J. Am. Ceram. Soc.* **79** [1] 51-57 (1996).
12. J. D. Helfinstine and S. T. Gulati, "Measurement of ultraslow crack growth in high silica glasses," abstract in *Ceram. Bull.*, **71** 470 (1992).
13. M. J. Matthewson, "Fiber lifetime predictions," *Proc. Soc. Photo-Opt. Instrum. Eng.* **1580** 130-141 (1991).
14. H. H. Yuce, P. L. Key and H. C. Chandan, "Aging behavior of low strength fused silica fibers," *Proc. Soc. Photo-Opt. Instrum. Eng.* **1366** 120-128 (1990).
15. "FOTP-28 - Method for measuring dynamic tensile strength and fatigue parameters of optical fibers by tension," TIA/EIA-455-28-C, Telecommunications Industry Association, Washington, DC, (1999).
16. G. M. Bubel and M. J. Matthewson, "Optical fiber reliability implications of uncertainty in the fatigue crack growth model," *Opt. Eng.* **30** [6] 737-745 (1991).
17. C. R. Kurkjian, J. T. Krause and M. J. Matthewson, "Strength and fatigue of silica optical fibers," *J. Lightwave Tech.* **7** 1360-1370 (1989).
18. D. R. Thoman, L. J. Bain and C. E. Antle, "Inferences on the parameters of the Weibull distribution," *Technometrics* **11** [3] 445-460 (1969).
19. T. Breuls and T. Svensson, "Strength and fatigue of zirconia induced weak spots in optical fiber," *Proc. Soc. Photo-Opt. Instrum. Eng.* **2074** 78-82 (1993).
20. M. J. Matthewson, C. R. Kurkjian and S. T. Gulati, "Strength Measurement of Optical Fibers by Bending," *J. Am. Ceram. Soc.* **69** 815 (1986).
21. M. J. Matthewson and C. R. Kurkjian, "Static fatigue of optical fibers in bending," *J. Am. Ceram. Soc.* **70** [9] 662-668 (1987).